A R C H I V E S O F M E T A L L U R G Y A N D M A T E R I A L S
Volume 60 2015 Issue 2
DOI: 10.1515/amm-2015-0108

J.H. KIM*, J.-H. LEE*,♯

GRAPHITE NANOSHEET EXFOLIATION FROM GRAPHITE FLAKES THROUGH FUNCTIONALIZATION USING PHTHALIC ACID

ZŁUSZCZANIE NANOARKUSZY GRAFITU Z PŁATKÓW GRAFITU PRZY UŻYCIU KWASU FTALOWEGO

In order to fabricate graphite nanosheets from graphite flakes, edge-functionalized graphite nanosheets were prepared by a functionalization method using phthalic acid as the molecule to be grafted. A polyphosphoric acid/P_2O_5 solution containing graphite and phthalic acid were heated at different temperatures for 72 h in a nitrogen atmosphere. It was confirmed by transmission electron microscopy and atomic force microscopy that the resultant phthalic acid-functionalized graphite nanosheets had a large surface area of 20.69 μm^2 in average and an average thickness of 1.39 nm. It was also found by X-ray diffractometry and Fourier transform infrared spectroscopy (FT-IR) analysis that the functionalization caused the formation of C=O bonds at the edges of the graphite nanosheets. The yield from this functionalization method was found to be dependent on the reaction temperature, only when it is between 70 and 130°C, because of the dehydration of phthalic acid at higher temperatures. This was confirmed by FT-IR analysis and the observation of low thermal energies at low temperatures.

Keywords: Exfoliation, Graphite nanosheet, Functionalization, Grafting molecule, Friedel-Crafts acylation

1. Introduction

Graphite is an allotrope of carbon and has a stacked lamellar structure of 2D networks of carbon atoms comprised of stable C-C covalent bonds. Due to its unique properties, graphite represents an important material in many existing and emerging technological applications requires non-reactivity. For example, this element is used in crucibles and susceptors [1,2]. Furthermore, the graphite lamellae or layers are bond through Van der Waals forces, which act along the common c-axis, and there happens to be a lot of interest currently in obtaining graphite nanosheets through exfoliation by overcoming these Van der Waals forces in graphite. Graphite nanosheets find several applications owing to their excellent electrical, mechanical, and thermal properties [3-10]. Aditionally, they are relatively inexpensive compared to carbon nanotubes and other carbon materials depending on the cost-effectiveness of their respective fabrication method/s [3,13-15].

The exfoliation methods typically employed can be classified into two categories: physical and chemical. The former involves the use of micromechanical cleavage to fabricate high-quality graphite nanosheets [16], but is not suitable for mass production as it is a labor-intensive method. The latter is more amenable to mass production industrially because it is a solution-based process [17-23]. However, the acid solutions used for chemical exfoliation are not eco-friendly, and additionally cause defects in the resultant graphite nanosheets. Besides, ultrasonication in acid solutions too has adverse effects on the nanosheets [23,24]. Thus, the average surface area of the resultant exfoliated nanosheets is generally small [13,14,25-27]. Therefore, a new process to exfoliate graphite nanosheets from graphite flakes that is eco-friendly, less destructive, efficient, and has high yields is urgently required. Baek et al. recently developed a novel process for the synthesis of graphite nanosheets through functionalization based on Friedel-Crafts acylation [28]. It was stated that this method is eco-friendly, does not introduce defects, and is appropriate for mass production. Nevertheless, we believe this process still requires more investigation into the applicability of different grafting molecules and reaction media, and the flexibility of process parameters (reaction temperature and time). Clarity concerning the efficiency of and the yield from this method is important too. Therefore, in this study, we explored phthalic acid, which has two carbonium ions, as a functionalizing agent. Additionally, the optimum process parameters for achieving the highest yield too have been investigated.

2. Experimental

Four grams each of phthalic acid (C_6H_4-1,2-$(CO_2H)_2$, >99.5%) and graphite flakes (>90%, +100 mesh (minimum >75%)) were added to mixture of 50 g of polyphosphoric acid (PPA, $H_{n+2}P_nO_{3n+1}$, >83%) and 12.5 g of phosphorus pentoxide (P_2O_5, 98%) in that order in a nitrogen atmosphere with constant stirring at different temperatures for 72 h. All chemicals were purchased from Sigma-Aldrich. The resultant pre-

* DEPARTMENT OF MATERIALS SCIENCE & ENGINEERING, SEOUL NATIONAL UNIVERSITY OF SCIENCE & TECHNOLOGY, SEOUL 139-743, REPUBLIC OF KOREA
♯ Corresponding author: pljh@snut.ac.kr

cipitate obtained after the reaction went through to completion was rinsed with distilled water and methanol. To remove the residual solvent, centrifugation was conducted several times at 7000 rpm for 15 min using distilled water. Residual phthalic acid too was removed by centrifugation under identical conditions using methanol (99.5%, Duksan Pure Chemicals). Subsequently, the final products were collected by drying under reduced pressure for 24 h.

The phthalic acid-functionalized graphite nanosheets were examined using transmission electron microscopy (TEM, Tecnai 20, FEI Co.). A homogeneous dispersion (supernatant), prepared by re-dispersing the phthalic acid-functionalized graphite nanosheets, was allowed to drip onto a copper grid and then dried to prepare TEM samples. To measure the thicknesses of 100 graphite nanosheets, a drop of the dispersion was placed on a silicon wafer and dried. The thickness of each nanosheet was quantitatively studied by tapping mode atomic force microscopy (AFM, Nanoscope IV, Digital Instrument). The graphite flakes were evaluated, before and after functionalization, by X-ray diffraction (XRD, X'pert MPD, Philips) analysis using CuK_{α} radiation. The chemical functional groups bonded to graphite were identified by Fourier transform infrared spectroscopy (FT-IR, Vertex 80v, Bruker Optics Co.).

We calculated the total yield of graphite nanosheets from the stated process (the mass of dispersed graphite nanosheet/the mass of initial graphite flake, $W_{nanosheet}$ / W_{flake}) as follows:

$$\frac{W_{nanosheet}}{W_{flake}} = \frac{W_{flake} - W_{sediment}}{W_{flake}}$$

Where $W_{sediment}$ represents the weight of the sediment in its dried state after centrifugation.

3. Results and discussion

Fig. 1 shows the TEM micrographs of a phthalic acid-functionalized graphite nanosheet along its plane and of a cross-section of it; the images were obtained in this study, and upon observation, the structures/artifacts observed in a typical nanosheet functionalized at 100°C. The average width and length of the wrinkled graphite nanosheets were estimated to be 5.36 μm ($\sigma \leqslant 1.16$ μm) and 3.86 um ($\sigma \leqslant 0.73$ μm), respectively. This shows that such a functionalization method can be used to fabricate graphite nanosheets larger than those obtained by previously reported methods [13,14,25-27], because PPA is a relatively mild acid and there is no sonication process involved. As shown in Fig. 1(b), the thickness of graphite nanosheets can be indirectly measured from their cross-sectional images. However, direct thickness measurement is required to obtain more quantitative results. We therefore measured the thickness of graphite nanosheets using AFM.

Fig. 2 is a histogram showing the number of graphite nanosheets in various thickness ranges, obtained through exfoliation by functionalization at 100°C. The average thickness of the graphite nanosheets was estimated to be 1.39 nm ($\sigma \leqslant$ 1.02 nm), which indicates that the average number of layers per nanosheet, given an average thickness of nanosheet of 0.34 nm, is approximately 4. Moreover, most of the 100 graphite nanosheets evaluated had less than 10 layers, and approximately 46% of them had less than 4 layers.

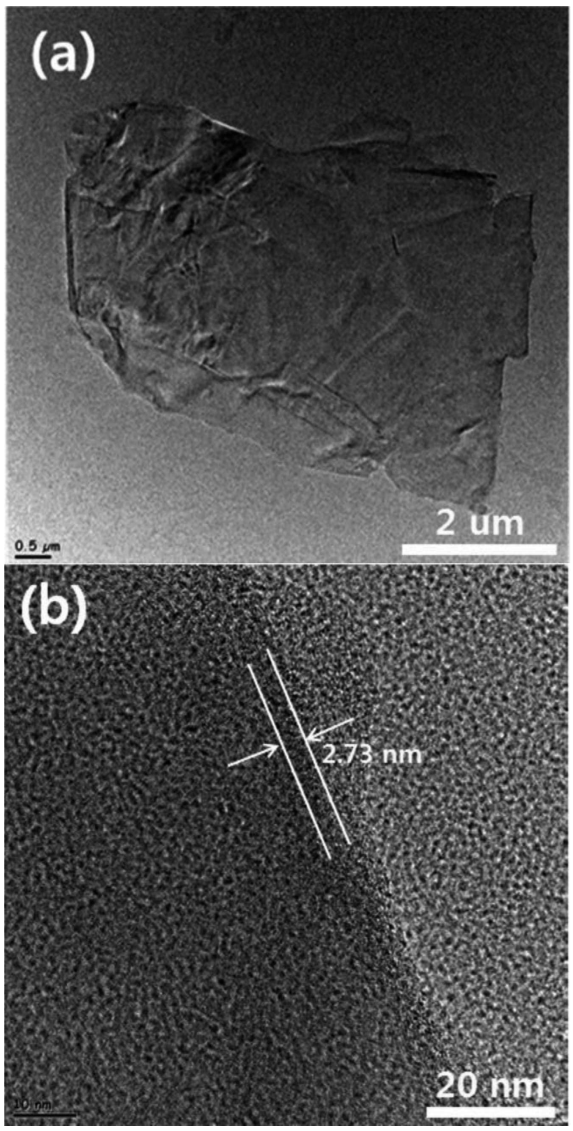

Fig. 1. Bright-field TEM micrographs showing (a) a plane and (b) a cross-sectional image of a phthalic acid-grafted graphite nanosheet, typically observed after functionalization at 100°C

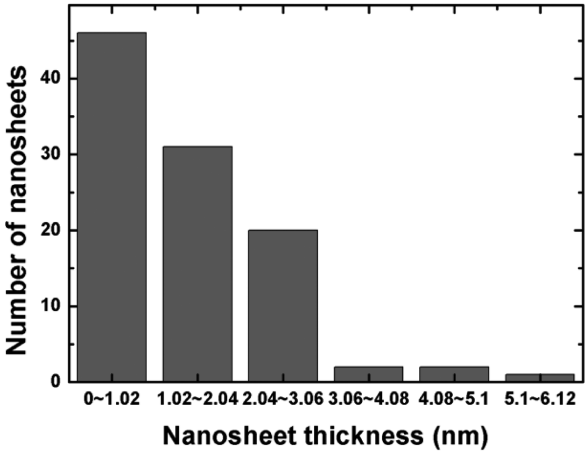

Fig. 2. Histogram showing the number of graphite nanosheets for various thickness ranges upon exfoliation by functionalization

These few-layer graphite nanosheets were exfoliated mainly through strong shearing forces caused by the viscous nature of PPA after functionalization with phthalic acid. The mechanism of functionalization of graphite using phthalic acid is shown in Fig. 3. Functionalization of graphite flakes by phthalic acid in the mildly acidic PPA/P_2O_5 medium occurs through an aromatic electrophilic substitution reaction [28]. The acidic nature of PPA causes protonation of the carboxyl group of phthalic acid. Electrons in the C-O bonding flow to the positively charged H_3O^+. Subsequently, P_2O_5 dehydrates phthalic acid causing generation of carbonium ions ($C{=}O^+$) from the phthalic acid. In these reactions, defect sites (mostly $C(sp^2)$-H/C=H), which are inherently present at the edges of graphite, host the electrophilic substitution reactions with the generated carbonium ions [29]. The homogenous grafting of phthalic acid onto the graphite edges across the basal plane without any damage to the crystalline structure is obtained through the mechanism of Friedel-Crafts acylation in the PPA/P_2O_5 medium. Post complete functionalization, the grafted phthalic acid exhibits ketone (C=O) bonding in its structure. In this mechanism, PPA is believed to play two important roles: one of dispersing medium and the other of aiding functionalization.

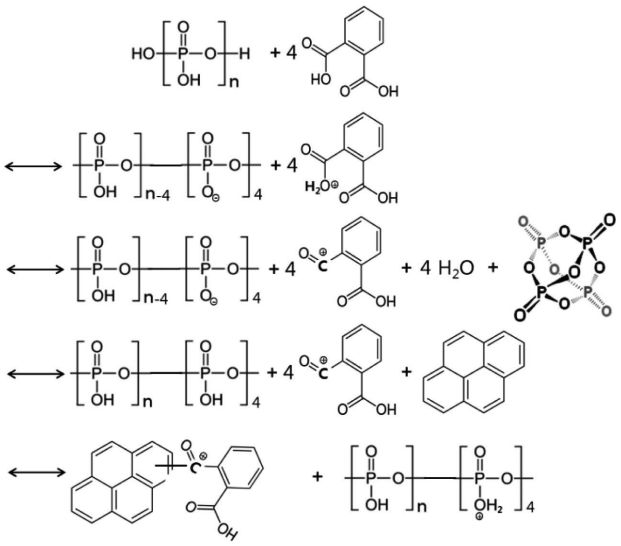

Fig. 3. Functionalization mechanism of graphite using phthalic acid

After functionalization, the phthalic acid-functionalized layers repel each other, opening a gap between them locally. Then, the viscous PPA infiltrates these gaps and causes strong shearing, thereby interrupting the restacking of the graphite nanosheets [29]. This shearing causes the gap to open up further. Additionally, PPA induces protonation of the surface of graphite nanosheets [29]. Subsequently, strong ionic interactions occur between the graphite surfaces. The functionalized graphite is thus completely exfoliated in the form of nanosheets.

In graphite, edge-selectively functionalized with phthalic acid, the interlayer spacing distance at the edges (d_{edge}) increases around the edge region because of the repulsive forces induced between the grafted molecules on each functionalized graphite layer [30]. Consequently, the interlayer spacing distance at the basal center of graphite (d_{center}) decreases to the relieve the stresses generated by increasing d_{edge}. These stresses are thus released to reduce the interlayer spacing of the regions farther from the edges. Hence, d_{center} decreases; the accompanying structural change was confirmed from the XRD patterns seen in Fig. 4. Fig. 4 shows the XRD patterns of pristine graphite and phthalic acid-functionalized graphite. The slight shifting of the (002) peak to a higher angle indicates the decrease in interplanar spacing (d value) [30]. The average value of d_{002} decreased from 0.3467 nm to 0.3442 nm after functionalization. This average d value was calculated using the 2θ angle associated with the (002) peak, as seen in Fig. 4(b), by Bragg's equation. Furthermore, the peak intensity from the (002) plane decreased evidently, suggesting that exfoliation had successfully occurred. With progressing exfoliation, the number of layers in each graphite flake decreased. Consequently, the interference between X-ray reflections from various planes in the graphite flakes decreased, and so did the intensities of XRD peaks.

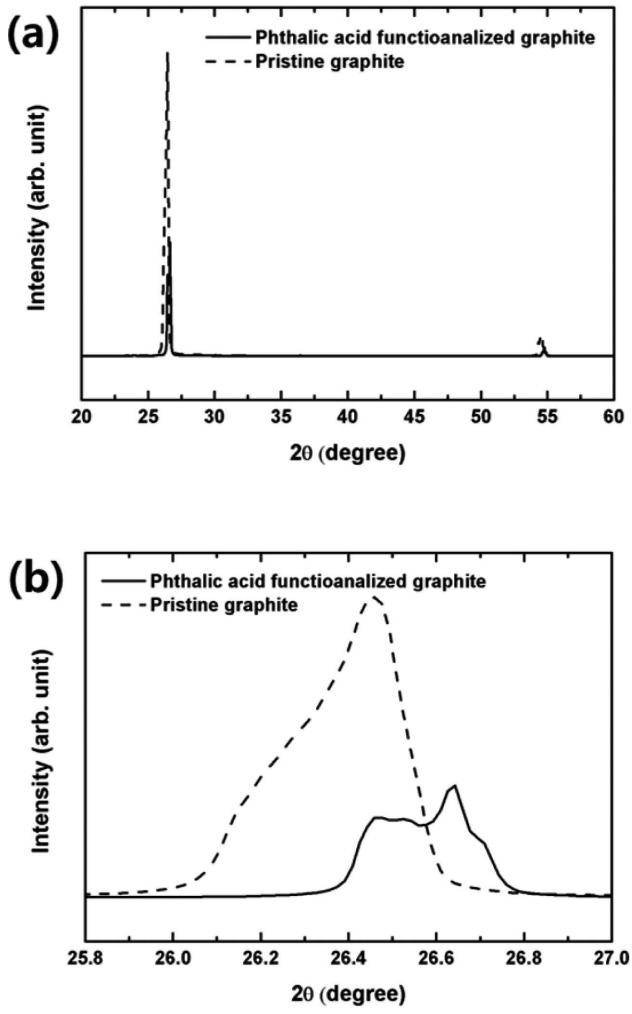

Fig. 4. (a) XRD patterns for the 2θ ranges of (a) 20.0-60.0o and (b) 25.8-27.0o of pristine graphite and phthalic acid-functionalized graphite

Fig. 5 shows the FT-IR spectra of phthalic acid and phthalic acid-functionalized graphite. The phthalic acid-functionalized graphite sample showed the presence of aromatic ketone C=O at 1710 cm^{-1}. However, the carboxylic C=O stretch at 1680 cm^{-1}, which is typically exhibited by pure phthalic acid, is evidently absent. These results show that the

Friedel-Crafts acylation reaction between phthalic acid and graphite flake occurred successfully at graphite edges [31].

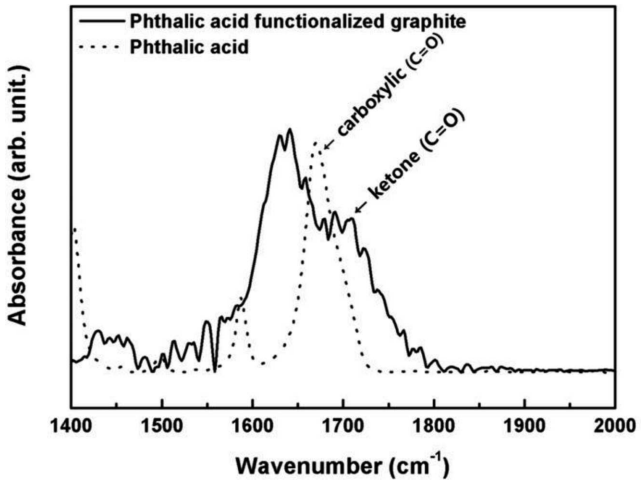

Fig. 5. FT-IR spectra of phthalic acid and phthalic acid-functionalized graphite

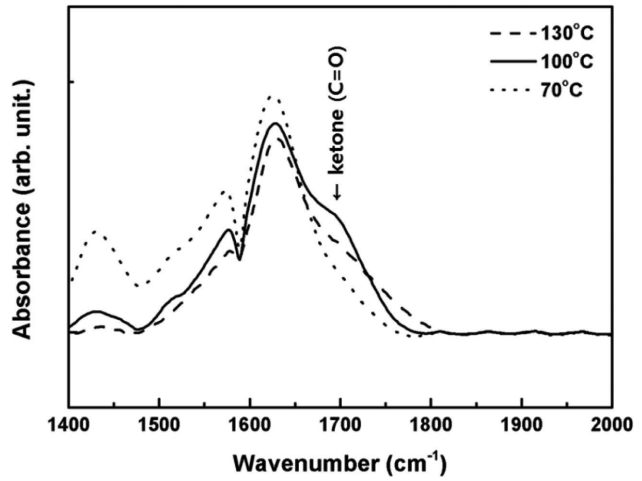

Fig. 6. FT-IR spectra of phthalic acid-functionalized graphite processed at different temperatures

In order to observe the effect of reaction temperature, we fabricated phthalic acid-functionalized graphite at different reaction temperatures. From the results shown in Table 1, it can be concluded that reasonable reaction temperature for obtaining high yields is 100°C. Considering its dehydration reaction, phthalic acid does not exhibit carboxylic C=O stretching for carboxylic acid at high temperatures. Hence, it can be inferred that the Friedel-Crafts acylation hardly occurs and the yield of functionalized graphite decreases with increasing reaction temperature. This tendency was confirmed by the FT-IR spectra. Fig. 6 shows the FT-IR spectra of phthalic acid-functionalized graphite processed at different temperatures. The aromatic ketone C=O absorbance at 1710 cm^{-1} increases with increasing reaction temperature from 70°C to 100°C. The absorbance decreases when the reaction temperature is increased further, from 100°C to 130°C. The Friedel-Crafts acylation occurred to a lower degree at 130°C than at 100°C because of the dehydration of phthalic acid. At 70°C, it is estimated that the thermal energy required for the functionalization reaction to proceed is insufficient. The absorbance of aromatic ketone C=O at 70°C therefore indicated the lowest value. In summary, the increased dehydration of phthalic acid at higher temperatures influences the efficiency of functionalization, and the yield of graphite nanosheets is evidently affected by the reaction temperature.

TABLE 1
Yield of graphite nanosheets as fabricated by functionalization method discussed in this study at different temperatures

Reaction temperature (°C)	Yield (%)
70	8.24
100	12.06
130	10.87

4. Conclusions

Through functionalization using phthalic acid, pristine graphite flakes were exfoliated into edge-functionalized graphite nanosheets. The average surface area of the resultant exfoliated nanosheets was 20.69 μm^2, a high value. Additionally, the average number of layers per nanosheet was estimated to be approximately 4, and most of the nanosheets were comprised of less than 10 layers. It was found by XRD and FT-IR analyses that the functionalization by phthalic acid forms C=O bonds at graphite edges. The yield of graphite nanosheets varied with the reaction temperature, tested in the range of 70-130°C. In the case of samples functionalized at high temperatures, the dehydration of phthalic acid hindered the Friedel-Crafts acylation. When the reaction temperature was low, the low thermal energy available did not quite aid the progress of functionalization efficiently.

Acknowledgements

The authors would like to thank Korean Basic Science Institute (KBSI) for the TEM, XRD, and FT-IR measurements.

REFERENCES

[1] Y. Song, Z. Yanmin, D. Gao, J. Guo, H.S. Kim, J. Kor. Powd. Met. Inst. **20**, 332 (2013).
[2] R.M. German, J. Kor. Powd. Met. Inst. **20**, 85 (2013).
[3] J. Li, M.L. Sham, J.-K. Kim, G. Marom, Compos. Sci. Technol. **67**, 296 (2007).
[4] L.M. Viculis, J.J. Mack, O.M. Mayer, H.T. Hahn, R.B. Kaner, J. Mater. Chem. **15**, 974 (2005).
[5] F.C. Fim, J.M. Guterres, N.R.S. Basso, G.B. Galland, J. Polym. Sci., Part A: Polym. Chem. **48**, 692 (2010).
[6] K. Kalaitzidou, H. Fukushima, L.T. Drzal, Carbon, **45**, 1446 (2007).
[7] S. Gupta, P.R. Manetena, J. Reinf. Plast. Compos. **29**, 2037 (2010).
[8] D. Cho, S. Lee, G. Yang, H. Fukushima, L.T. Drzal, Macromol. Mater. Eng. **290**, 179 (2005).
[9] Y.C. Li, S.C. Tjong, R.K.Y. Li, Synth. Met. **160**, 1912 (2010).
[10] B. Debelak, K. Lafdi, Carbon, **45**, 1727 (2007).
[11] A. Mills, M. Farid, J.R. Selman, S. Al-Hallaj, Appl. Therm. Eng. **26**, 1652 (2006).

[12] J. Li, J.-K. Kim, Compos. Sci. Technol. **67**, 2114 (2007).
[13] A. Yu, P. Ramesh, M.E. Itkis, E. Bekyarova, R.C. Haddon, J. Phys. Chem. C **111**, 7565 (2007).
[14] S. Stankovich, D.A. Dikin, R.D. Piner, K.A. Kohlhaas, A. Kleinhammes, Y. Jia, Y. Wu, S.T. Nguyen, R.S. Ruoff, Carbon **45**, 1558 (2007).
[15] J. Shen, Y. Hu, C. Li, C. Qin, M. Ye, Small, **5**, 82 (2009).
[16] K.S. Novoselov, A.K. Geim, S.V. Morozov, D. Jiang, T. Zhang, S.V. Dubonos, I.V. Grigorieva, A.A. Firsov, Science **306**, 666 (2004).
[17] T. Wei, Z. Fan, G. Luo, C. Zheng, D. Xie, Carbon, **47**, 313 (2008).
[18] S. Malik, A. Vijayaraghavan, R. Erni, K. Ariga, I. Khalakhan, J.P. Hill, Nanoscale **2**, 2139 (2010).
[19] W. Gu, W. Zheng, X. Li, H. Zhu, J. Wei, Z. Li, Q. Shu, C. Wang, K. Wang, W. Shen, F. Kang, D. Wu, J. Mater. Chem. **19**, 3367 (2009).
[20] W. Fu, J. Kiggans, S.H. Overbury, V. Schwartz, C. Liang, Chem. Commun. **47**, 5265 (2011).
[21] A. Safavi, M. Tohidi, F.A. Mahyari, H. Chahbaazi, J. Mater. Chem. **22**, 3825 (2012).
[22] C. Valles, C. Drummond, H. Saadaoui, C.A. Furtado, M. He, O. Roubeau, L. Ortolani, M. Monthioux, A. Penicaud, J. Am. Chem. Soc. **130**, 15802 (2008).
[23] Y. Hernandez, V. Nicolosi, M. Lotya, F.M. Blighe, Z. Sun, S. De, I.T. McGovern, B. Holland, M. Btrne, Y.K. Gunko, R. Goodhue, J. Hutchison, V. Scardaci, A.C. Ferrari, J.N. Coleman, Nat. Nanotechnol. **3**, 563 (2008).
[24] D.A. Heller, P.W. Barone, M.S. Strano, Carbon **43**, 651 (2005).
[25] S. Stankovich, D.A. Dikin, G.H.B. Dommett, K.M. Kolhaas, E.J. Zimney, E.A. Stach, R.D. Piner, S.T. Nguyen, R.S. Ruoff, Nature **442**, 282 (2006).
[26] W. Qian, R. Hao, Y. Hou, Y. Tian, C. Shen, H. Gao, X. Liang, Nano Res. **2**, 706 (2009).
[27] S. Stankovich, R.D. Piner, S.T. Nguyen, R.S. Ruoff, Carbon **44**, 3342 (2006).
[28] E.-K. Choi, I.-Y. Jeon, S.-Y. Bae, H.-J. Lee, H.S. Shin, L. Dai, J.-B. Baek, Chem. Commun. **46**, 6320 (2010).
[29] D.W. Chang, H.-J. Choi, I.-Y. Jeon, J.-B. Baek, Chem. Rec. **13**, 224 (2013).
[30] J.-S. Park, M.-H. Lee, I.-Y. Jeon, H.-S. Park, J.-B. Baek, H.-K. Song, ACS Nano **6**, 10770 (2012).
[31] H.-J. Lee, S.-J. Oh, J.-Y. Choi, J.W. Kim, J. Han, L.-S. Tan, J.-B. Baek, Chem. Mater. **17**, 5057 (2005).

Received: 20 November 2014.